DOI: 10.1002/ejic.200801222

High-Pressure–High-Temperature Behavior of ζ-Fe_2N and Phase Transition to ε-$Fe_3N_{1.5}$

Ulrich Schwarz,[a] Aron Wosylus,[a] Michael Wessel,[b] Richard Dronskowski,[b] Michael Hanfland,[c] Dieter Rau,[d] and Rainer Niewa*[d]

Keywords: Iron / Nitrides / High-pressure chemistry / Ab-initio calculations / X-ray diffraction

Under the high-pressure–high-temperature conditions of a resistivity-heated Walker-type two-stage multi-anvil device [1600(200) K and 15(2) GPa] ζ-Fe_2N is transformed to single-crystalline ε-Fe_3N_{1+x} (x = 0.5). The crystal structure was refined in space group $P6_322$ [a = 4.8016(2) Å, c = 4.4269(2) Å, Z = 2, $R(F)$ = 1.27 %] resulting in a composition of $Fe_3N_{1.47(1)}$, i.e., under the selected preparation conditions the structural change takes place under conservation of the nitrogen content within experimental error. The applied pressure is necessary to prevent decomposition and formation of elemental nitrogen at elevated temperatures. Application of pressure in a diamond anvil cell at ambient temperature without external heating gives no indication of a phase transition of the starting material. A least-squares fit of a Murnaghan-type equation of state to the experimental pressure-volume data up to 25 GPa results in a compressibility of B_0 = 162.1(8) GPa, B_0' = 5.24(8), with V_0 = 118.09(1) Å^3. Density-functional electronic-structure calculations on ζ-Fe_2N and ε-Fe_2N for 0 K indicate that no pressure-induced phase transition can occur such that the phase transition must be driven by temperature, as is observed in the experiments. The bulk module for ζ-Fe_2N (B_0 = 219 GPa, B_0' = 4.46 GPa) is in acceptable agreement with the experimental results. Similar to the case of ε-$Fe_3N_{1.1}$, ε-$Fe_3N_{1.5}$ may be described both in space group $P312$ and $P6_322$, and again space group $P312$ is favored by 12.1 kJ/mol.

Introduction

Iron nitrides were discovered in the mid 19th century[1,2] and are studied intensively since then due to their refractory properties and their potential as attractive magnetic recording materials.[3,4] Additionally, thermodynamically not favored in oxygen containing atmospheres, nitrides are rare but present in the earth's crust at volcano craters due to limited oxygen supply for iron oxide formation (Fe_5N_2, Silvestrite also called Siderazote)[5] or originating from meteorites (Roaldite, Fe_4N).[6] Due to the abundance of nitrogen in deeper earth's regions, speculations on iron nitrides as components of the core were formulated and indeed furnish an improved description of the elastic properties.[7]

The binary system Fe–N contains a number of phases highly relevant to iron and steel hardening: In nitrogen atmosphere at elevated temperatures, iron forms a ferromagnetic γ′-Fe_4N phase in a limited range of homogeneity, stable only below 953 K. It presents an inverse perovskite structure in which the iron atoms arrangement is *fcc* and the nitrogen atoms occupy one-quarter of the octahedral interstices in a fully ordered manner.[8,9] In the ideal model of the crystal structure of ε-Fe_3N, one-third of the octahedral voids are occupied by nitrogen atoms within a hexagonal close-packed (*hcp*) arrangement of Fe. In this arrangement, NFe_6 octahedra share common vertices.[9] However, the ε-type iron nitride is known to exhibit a large homogeneity range,[10,11] a fact which can be already taken as an indication for some sort of nitrogen disorder. ζ-Fe_2N, also with a small homogeneity range, crystallizes in an inverse variant of the α-PbO_2-type structure. The iron atoms realize the motif of a slightly distorted *hcp* array with one-half of the octahedral interstices in each layer occupied by nitrogen species. The symmetry of the nitrogen arrangement is orthorhombic with space group *Pbcn*, and in each layer the nitrogen atoms are distributed in zigzag chains parallel to the orthohexagonal *b* axis.[12,13] Two additional binary iron nitride phases do not appear in the reported phase diagrams: The nitrogen richest material, γ′′-FeN, realizes a zinc blende-type structure and has so far been only prepared as thin films by reactive sputter deposition.[14–16] α′′-$Fe_{16}N_2$ is considered a material of importance which is the subject of controversies concerning the existence of a giant magnetic moment.[17]

Recently, we have presented the first preparation of single crystals of ε-$Fe_3N_{1\pm x}$ by a high-temperature–high-pressure

[a] Max-Planck-Institut für Chemische Physik fester Stoffe, Nöthnitzer Straße 40, 01187 Dresden, Germany
[b] Institute of Inorganic Chemistry, RWTH Aachen University, Landoltweg 1, 52056 Aachen, Germany
[c] European Synchrotron Radiation Facility, 38043 Grenoble, France
[d] Department Chemie, Technische Universität München, Lichtenbergstraße 4, 85474 Garching, Germany
Fax: +49-89-289-13762
E-mail: rainer.niewa@mytum.de

technique. The crystallization started either from ε-Fe_3N_{1+x}[18] or proceeded via a phase-transition of the starting material γ′-Fe_4N.[19] Here, we discuss the pressure-induced transformation of ζ-Fe_2N into ε-Fe_3N_{1+x} and the stability relations of the phases at elevated temperatures and pressures. Additionally, we present single-crystal X-ray diffraction data of ε-$Fe_3N_{1.5}$ as obtained by transformation of ζ-Fe_2N.

Results and Discussion

The phase ε-Fe_3N is known to adopt nitrogen contents which can be significantly lower or higher than the nominal 3:1 composition, while the homogeneity range of ζ-Fe_2N is quite narrow.[10,11] Additionally, the stability range of ζ-Fe_2N is not well established with respect to temperature. In earlier publications we have reported the preparation of single crystals ε-Fe_3N_{1+x} with x = –0.05[19] and x = 0.08[18] by a high-temperature–high-pressure technique and discussed the nitrogen ordering within the *hcp* arrangement of iron with special focus on the two space groups $P6_322$ and $P312$. The combination of experimental data and results from quantum mechanic computations led us to the conclusion that the preferred structure model should be described in space group $P312$ for the studied samples. Now we are able to produce single crystals of the ε-Fe_3N homogeneity range with a significant higher nitrogen content from high-temperature–high-pressure treatment of ζ-Fe_2N resulting in ε-$Fe_3N_{1.5}$.

High-pressure–high-temperature treatment of ζ-Fe_2N (33.3 atom-% N) at p = 15(2) GPa and T = 1600(200) K yields a sample with ε-type ordering according to X-ray powder diffraction. Figure 1 shows the X-ray powder diffraction patterns prior and after the pressure experiment. Unit cell refinements converge at values of a = 4.797 Å and c = 4.419 Å for the material after treatment. This compares to a = 4.791 Å and c = 4.419 Å for a microcrystalline sample reported with the composition $Fe_3N_{1.39}$ (i.e., 31.7 at% N).[20] The product is completely re-crystallized, and suitable single crystals for X-ray diffraction experiments could be isolated from the product. The refinements of the intensity data led to a composition of $Fe_3N_{1.47(1)}$ (32.9 at% N). As was pointed out earlier, the maximum nitrogen content of ε-Fe_3N_{1+x} (without application of external pressure) was determined to x = 0.48 with only slight temperature dependence. For larger x a two-phase region separates the ε- and ζ-phases.[11,20,21] The unit cells of ζ- and ε-type phases show a simple geometric relation according to $a_\zeta \approx c_\varepsilon$; $b_\zeta \approx a_\varepsilon \times 2/\sqrt{3}$; $c_\zeta \approx a_\varepsilon$, however, the transition between both crystal structures involves a re-arrangement of nitrogen atoms by diffusion within the host of closed packed iron. The reason for the close proximity of the unit cells (and diffraction patterns) is the fact that in both crystal structures, the ζ- and the ε-type, the ordering of nitrogen is based on the occupation of octahedra in an array of hexagonal close-packed iron atoms. No simple symmetry relation paces way for a displacive phase transition. In Figure 2, we compare idealized crystal structure models of both phases which are depicted as frameworks of occupied octahedra within an identical array of Fe atoms. NFe_6 octahedra in ζ-Fe_2N share both common edges and vertices, those in ε-Fe_3N in the ideal structure (exact composition and no disorder) are connected exclusively via vertices, thus maximizing the distances between nitrogen atoms. Additional octahedral voids must consequently be occupied for a composition of $Fe_3N_{1.5}$ (see below).

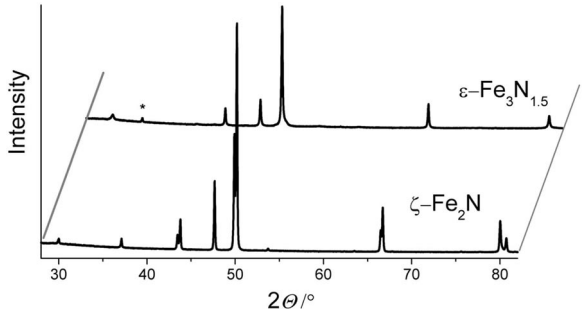

Figure 1. X-ray powder diffraction diagrams (taken with Co-$K_{\alpha 1}$ radiation) of ζ-Fe_2N (lower curve) and the product of the high-pressure–high-temperature treatment in the multi-anvil cell showing the pattern expected for a phase with ε-type order (one reflection of a small BN impurity from the crucible material is indicated by an asterisk). The horizontal shift of the pattern is shown by thin lines.

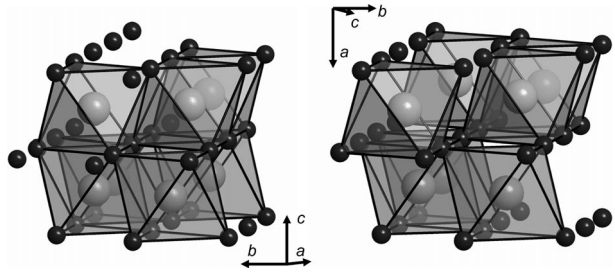

Figure 2. Crystal structures of ε-$Fe_3N_{1.5}$ (left) in the ordered variant (space group $P312$) and the arrangement of ζ-Fe_2N (right). Shaded octahedra are occupied by nitrogen in an identical array of iron forming the motif of a hexagonal close packing.

Structure refinements of the product ε-Fe_3N_{1+x} based on single-crystal X-ray diffraction data were performed in both considered structure models in $P6_322$ and $P312$. Table 1 gives results of structure refinements in $P6_322$. The ideal structure for the ε-type structure with composition Fe_3N would have Wyckhoff position 2*c* fully occupied, whereas all other octahedral voids in the *hcp* arrangement of Fe remain unoccupied. This model results in a framework of all vertex-sharing $NFe_{6/2}$ octahedra. However, for phases with nitrogen contents close to this composition we have shown a significant transfer of nitrogen from site 2*c* to the site 2*b* (about 10%),[18,19] which is probably entropy driven. For the presented composition with much higher nitrogen content, the 2*c* site is almost completely occupied. Structure refinements in $P6_322$ reveal an approximately 50% occupation of site 2*b* leading to the refined composition of ε-$Fe_3N_{1.47(1)}$. Figure 2 depicts the ideal crystal structure for

Table 1. Crystal structure parameters for ε-$Fe_3N_{1.47(1)}$, values for displacement parameters U are given in Å^2.

Atom	Site	x	Y	z	Occ.	U_{eq}
Fe	6*g*	0.33200(4)	0	0	1	0.00595(2)
N(1)	2*c*	1/3	2/3	1/4	0.993(4)	0.0075(2)
N(2)	2*b*	0	0	1/4	0.479 (7)	0.0048(6)
Atom	U_{11}	U_{22}	U_{33}	U_{23}	U_{13}	U_{12}
Fe	0.00613(4)	0.00628(6)	0.00550(4)	0.00148(3)	1/2 U_{23}	1/2 U_{22}
N(1)	0.0077(3)	U_{11}	0.0070(5)	0	0	1/2 U_{11}
N(2)	0.0054(6)	U_{11}	0.004(1)	0	0	1/2 U_{11}

ε-Fe_3N with the structural model of $Fe_3N_{1.5}$. Here, the octahedra around the 2*b* site share edges with the aforementioned framework forming parallel rods of face-sharing octahedra oriented along [001]. The observed 50% occupation would allow for an ordered occupation of every second octahedra avoiding large repulsive interactions between nitrogen species. Since no superstructure reflections were observed, a symmetry reduction has to be performed into a translation equivalent space group, leading to *P*312 with a fully ordered nitrogen substructure. However, refinements of this model lead to a composition with clearly reduced nitrogen content and large residuals in the final electron difference map in the respective unoccupied position. These facts in combination with earlier observations lead us to the following interpretation: The rods of face-sharing octahedra with occupation of 50% are internally ordered for energy reasons (minimizing Coulomb repulsion between neighboring face-sharing octahedra), but the interaction of parallel rods is not sufficiently high for a fully three-dimensional ordering of these rods,[22] compare Figure 3. A clear discrimination of both space groups would be possible from X-ray diffraction data with the extinction condition of (00*l*) with $l = 2n + 1$ forbidden in $P6_322$, but allowed in *P*312. However, even for the fully ordered structure of $Fe_3N_{1.5}$ in *P*312 the strongest reflection in question with $l = 3$ in the accessible 2-theta range calculates to an intensity of less than 0.03% of the strongest reflection (002).

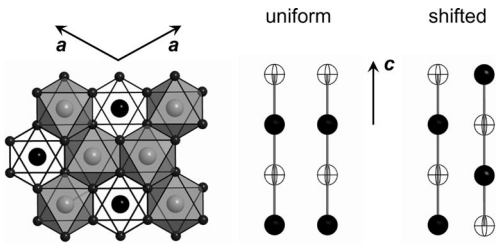

Figure 3. Possible ordered arrangements of nitrogen on position 2*b* (space group $P6_322$) in ε-Fe_3N_{1+x} for $x = 0.5$. Left: view along [001]. Framework of vertex-sharing fully occupied NFe_6 octahedra (site 2*c*, grey octahedra) and orientation of rods of internally face-sharing octahedra occupied to 50% (site 2*b*, open octahedra). Right: neighboring rods can be orientated either uniform or shifted (according to T. Epicier).[35] The first choice is the only possibility for a completely ordered structure in the given unit cell, the second choice would lead to structural frustration due to the trigonal motif.

Distances *d*(Fe–N) with 1.9485(1) Å for the fully occupied site N(1) and 1.9407(2) Å for the 50% occupied position N(2) are in the range of other iron nitrides.[13,18,19,20] Compared to phases of the ε-Fe_3N phase field with lower nitrogen content,[18,19] these distances become larger and progressively more similar with increasing nitrogen content.

Although the X-ray diffraction patterns of ζ-type and ε-type ordered materials are very similar (compare also with Figure 1, showing the ambient pressure X-ray diffraction patterns of ζ-Fe_2N and ε-$Fe_3N_{1.5}$), the discrimination of the phases in in-situ high-pressure X-ray diffraction could be carried out unambiguously: Figure 4 shows selected X-ray powder diffraction data at different pressures. Due to the orthorhombic distortion of the underlying motif of a hexagonal close packing of Fe, the pattern of ζ-Fe_2N shows several split reflections compared to that of the ε-phase. The splitting vanishes at increased pressures due to reflection broadening; however, the affected reflections still exhibit shoulders or a larger full-width at half-maximum. Additionally, two weak reflections at low diffraction angles are present in all patterns up to highest pressures indicating the presence of the ζ-phase, while one weak reflection of the ε-phase calculated to be visible at a different angle does not grow from the background. As a conclusion, in-situ high pressure X-ray diffraction at ambient temperature in a diamond anvil cell using synchrotron radiation evidences that ζ-Fe_2N remains stable up to 25 GPa.

For a theoretical insight into the driving forces of the phase transition, several structure models of Fe_2N were calculated by density-functional electronic-structure calculations at 0 K (Table 2). It is found that ζ-Fe_2N (*Pbcn*) is an exothermic phase compared to the elements (ΔH = –12.1 kJ/mol; exp: –3.8 kJ/mol).[23] Similar to the case of ε-$Fe_3N_{1.1}$, ε-$Fe_3N_{1.5}$ may be described in both space group *P*312 and $P6_322$, and again space group *P*312 is favored, in this case by –12.1 kJ/mol. Both ε-Fe_2N structures lie higher in energy than ζ-Fe_2N, and they also have a lower density such that a pressure-driven phase transition can be ruled out.

Figure 5 depicts the unit cell volume as a function of pressure. A Murnaghan-fit[24] results in a compressibility of B_0 = 162.1(8) GPa, B_0' = 5.24(8), V_0 = 118.09(1) Å^3 being very close to that of the related material ε-Fe_3N_{1+x} (x = 0.08) with B_0 = 172(4) GPa and B_0' = 5.7 (fixed).[18] The theoretical course of the volumes and the calculated bulk modulus of ζ-Fe_2N [B_0 = 220(4) GPa, B_0' = 4.4(1), V_0 =

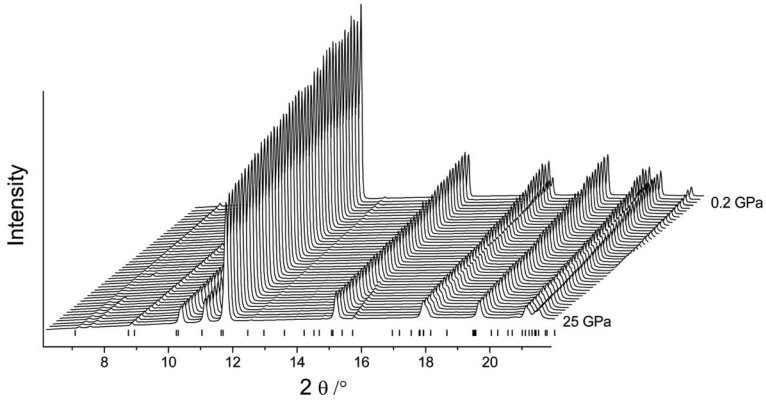

Figure 4. X-ray powder diffraction patterns taken on ζ-Fe_2N with synchrotron radiation (41.3 pm) at different pressures in a DAC. The superstructure reflections at low angles and the splitting of the profiles at approximately 18° indicate the conservation of ζ-type ordering up to at least 25 GPa.

Table 2. Density-functional total-energy results of different crystal structure models for ζ- and ε-type Fe_2N with space group *Pbcn* as reference point for enthalpy and volume.

	Δ*H* [kJ/mol]	Δ*V* [Å^3]	B_0 [GPa]	B_0' [GPa]
Pbcn (ζ-Fe_2N)	0.00	0.00	219	4.46
*P*312 (ε-$Fe_3N_{1.5}$)	15.3	0.11	210	4.66
$P6_322$ (ε-$Fe_3N_{1.5}$)	27.4	0.26	217	4.36
2Fe + α-N	12.1	20.96	–	–

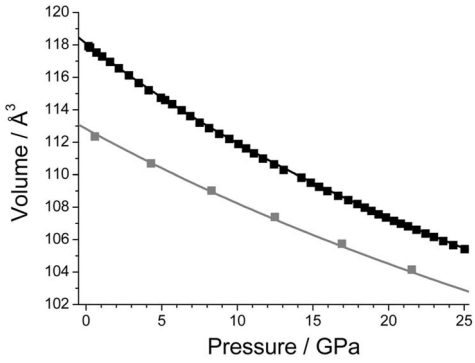

Figure 5. Pressure–volume data of ζ-Fe_2N. The black solid line is the result of a least-squares refinement of a Murnaghan-type equation of state to the experimental data (black squares). The corresponding curve for the data obtained by band structure calculations (grey squares) is shown in grey.

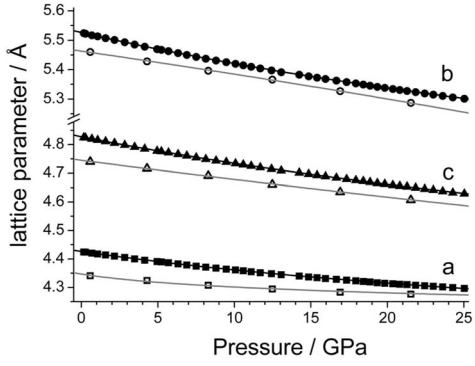

Figure 6. Pressure dependence of the lattice parameters of the orthorhombic unit cell of ζ-Fe_2N. Open symbols show results of the density-functional calculations, full symbols are experimental data; lines represent least-squares fits of Murnaghan-type equations of state to the data.

112.8(1)] is in acceptable agreement with the experimental observations. The anisotropic compression of the different crystallographic directions of the orthorhombic unit cell is shown in Figure 6.

Conclusions

We have successfully transformed ζ-Fe_2N into ε-Fe_3N_{1+x} (x = 0.5) under high-pressure–high-temperature conditions realized in an internally heated Walker-type two-stage multi-anvil device. At the selected conditions, the structural change takes place under conservation of the nitrogen content within experimental error. The transformation may not be directly influenced by the applied pressure in the sense of a thermodynamically changed stability, but the external compression certainly helps to avoid nitrogen losses and, thus, prevents decomposition. This is indirectly supported by the finding that application of pressure alone in a diamond anvil cell at ambient temperature gives no indication of a phase transition of the starting material. The high value of the bulk modulus is in accordance with the character of a hard material. Our ab initio calculations give no indication for a pressure-induced phase transition from ζ-Fe_2N into ε-$Fe_3N_{1.5}$, leaving temperature as the most likely driving parameter. The bulk modulus as calculated using density functional theory is in acceptable agreement with the experimental observations.

Experimental Section

Preparation and Characterization: Single phase microcrystalline samples ζ-Fe_2N were prepared by reaction of iron powder (99.9%, Johnson Matthey/Alfa) with flowing NH_3 (99.98% NH_3) at 435 °C using a flow of 20 sccm (sccm is the gas volume flow in cm^3 under standard conditions, 1.013 bar, per minute) in a tube with a diameter of about 5 cm.

Chemical analyses on O, N and H were performed using the carrier gas hot-extraction technique with a LECO analyzer TCH-600. All values are averages of at least 3 independent measurements. Chemical analysis of the starting material results in a composition of $Fe_2N_{0.986\pm6}O_{0.0252\pm8}$ [w(O) = 0.32 ± 0.01%, w(N) =

10.97 ± 0.07%]. Hydrogen impurities were below the detection limit of 0.008% in all measurements.

X-ray powder diffraction experiments in the laboratory were carried out using an Imaging Plate Guinier Camera (HUBER diffraction, Co-$K_{\alpha1}$ radiation, 6 × 15 min scans, $8° \leq 2\Theta \leq 100°$). X-ray diffraction intensity data on a single crystal were collected on a STOE IPDS diffractometer using graphite-monochromated Ag-K_α radiation. The structure was solved and refined with the SHELX package of programs.[38, 39] Table 3 gives crystallographic data and information concerning the measurement.

Table 3. Crystallographic data of ε-$Fe_3N_{1.47(1)}$.

Space group	$P6_322$
Refined formula	$Fe_3N_{1.47(1)}$
a [Å]	4.8016(2)
c [Å]	4.4269(2)
V [Å^3]	88.39
Z	2
$D_{calcd.}$ [g cm^{-3}]	7.069
μ(Ag-K) [mm^{-1}]	12.26
F(000) [e]	176.6
hkl range	–12–7, –7–12, –11–6
$2\theta_{max}$ [°]	90
Reflections measured	1747
Reflections unique	498
R_{int}	0.0134
Parameters refined	13
$R(F)$ [$F_o > 4\sigma(F_o)$]	0.0127
$R(F)$/w$R(F^2)$ (all reflections)	0.0404/0.0247
GoF(F^2)	1.033
$\Delta\rho_{max}$ [e Å^{-3}]	1.16

Further details of the crystal-structure investigation may be obtained from the Fachinformationszentrum Karlsruhe, 76344 Eggenstein-Leopoldshafen, Germany, on quoting the depository number CSD-420214.

High-Pressure Synthesis Experiments and Characterization: High-pressure conditions are realized with a hydraulic uniaxial press. Force redistribution in order to achieve quasi-hydrostatic conditions is accomplished by a Walker-type module (two-stage assembly with a central octahedral pressure chamber)[25–28] and MgO/Cr_2O_3 octahedra with an edge length of 14 or 18 mm. Elevated temperatures are realized by resistive heating of graphite tubes containing the sample crucible. Pressure and temperature calibration is completed before the experiments by analyzing the resistance changes of bismuth and lead[29] and measuring set-ups equipped with a W/WRe thermocouple, respectively. The crucibles girdling the sample mixtures are made from hexagonal boron nitride. X-ray powder diffraction data and energy dispersive X-ray analysis do not give evidence for a reaction of the container with the sample. Thus, separation of reaction products and crucible material can be achieved easily. A typical high-pressure synthesis requires pressure increase for 3 h, holding at the maximal pressure for typically 5 h followed by pressure decrease in 10 h. During maximum pressure of 15(2) GPa the samples were heated to 1600(200) K for 5 min. Heated samples are quenched to ambient temperature by disconnecting the heating current before decompression. Products were shiny grayish-black compact cylindrical ingots with conchoidal fracture behavior.

In-Situ Diffraction Experiments at High Pressures: Iron nitride ζ-Fe_2N was ground into a fine powder and placed in steel gaskets using helium as a pressure transmitting medium. High pressures were generated by diamond anvil cells and determined by the ruby luminescence method. X-ray powder diffraction experiments were carried out at the undulator beamline ID 9A of the ESRF, Grenoble. During the exposures samples were oscillated by ±3° in order to enhance powder statistics. Typical exposure times were two to five seconds. The diffraction patterns were collected on an imaging plate detector which is positioned at a distance of approximately 450 mm from the sample. For calibration of wavelength (41.3 pm) and detector distance we used a silicon sample. Integration of the two-dimensional raw data was performed using the pattern integration software image integrator.[30] Peak positions and lattice parameters were refined using the computer program WinCSD.[31]

Electronic Structure Calculations: The ab initio calculations are based on the plane wave/pseudopotential strategy using the computer program VASP (Vienna Ab initio Simulation Package)[32,33] employing the generalized gradient approximation (GGA) of the PBE type[34] and the projected-augmented wave (PAW) method.[35] A cut-off energy of 500 eV and a dense net of k-points was chosen to find the optimum structure lying lowest in energy. For a correct simulation of ε-Fe_2N in both space groups $P312$ and $P6_322$ the supercell approach was used. To do so, a cell of ε-Fe_3N was doubled both in x and y directions, and four nitrogen atoms were carefully added so that the symmetry did match the required one. In addition, the unit cells were allowed to change in volume and shape, and all atomic positions were allowed to relax. Because of the small energy differences the convergence criterion of the electronic structure calculation was set to 0.01 meV. This method has been successfully used for other ternary iron nitrides[36,37] prior to their synthesis. After finding the cell lowest in energy for each structure and composition, the volume was changed around the ambient pressure equilibrium value and bulk modules were obtained by fitting Murnaghan-type equations of state to the calculated energy-volume data.

Acknowledgments

We thank Anja Völzke for performing the chemical analyses. Additionally we wish to acknowledge the assignment of beamtime at the undulator beamline ID09A of the ESRF. We also thank the computer center of RWTH Aachen University and the Jülich supercomputing center for the possibility to use their computer resources. This work was supported by the Elitenetzwerk Bayern within the Advanced Materials Science program, the Max-Planck-Gesellschaft, and within the Schwerpunktprogramm "Synthesis, in-situ characterisation, and quantum mechanical modelling of Earth Materials, oxides, carbides and nitrides at extremely high pressures and temperatures" of the Deutsche Forschungsgemeinschaft (DFG) (SPP 1236).

[1] C. Despretz, *Ann. Chim. Phys.* **1829**, *42*, 122.
[2] C. L. Berthollet, L. J. Thénard, *Traité Chim.* **1834**, *1*, 434.
[3] A. Fry, *Stahl Eisen* **1923**, *43*, 1271–1279.
[4] D. Andriamandroso, L. Fefilatiev, G. Demazeau, L. Fournès, M. Pouchard, *Mater. Res. Bull.* **1984**, *19*, 1187–1194.
[5] O. Silvestri, *Poggendorfs Annalen der Physik und Chemie* **1867**, *157*, 165–172.
[6] V. F. Buchwald, H. P. Nielsen, *Lunar Planet. Sci.* **1981**, *12*, 112–114.
[7] J. F. Adler, Q. Williams, *J. Geophys. Res.* **2005**, *110*, B01203.
[8] K. H. Jack, *Proc. R. Soc. London, Ser. A* **1948**, *195*, 34–41.
[9] H. Jacobs, D. Rechenbach, U. Zachwieja, *J. Alloys Compd.* **1995**, *277*, 10–17.
[10] K. H. Jack, *Proc. R. Soc. London, Ser. A* **1951**, *208*, 200–215.
[11] H. A. Wriedt, N. A. Gokcen, R. H. Nafziger, *Bull. Alloy Phase Diagrams* **1987**, *8*, 355–377 and references given therein.

[12] D. H. Jack, K. H. Jack, *Mater. Sci. Eng.* **1973**, *11*, 1–27.
[13] D. Rechenbach, H. Jacobs, *J. Alloys Compd.* **1996**, *235*, 15–22.
[14] M. Takahashi, H. Fujii, H. Nakagawa, S. Nasu, F. Kanamaru, *Proc. 6th Int. Conf. Ferrites*, Tokyo and Kyoto, Japan, **1992**, 508.
[15] S. Kikkawa, T. Yamamoto, K. Ohta, M. Takahashi, F. Kanamaru, in: *The Chemistry of Transition Metal Carbides and Nitrides* (Ed.: S. T. Oyama), Blackie A & P – Glasgow, **1996**, p. 175.
[16] K. Suzuki, H. Morita, T. Kaneko, H. Yoshida, H. Fujimori, *J. Alloys Compd.* **1993**, *201*, 11–16.
[17] T. K. Kim, M. Takahashi, *Appl. Phys. Lett.* **1972**, *20*, 492–494.
[18] R. Niewa, D. Rau, A. Wosylus, K. Meier, M. Hanfland, M. Wessel, R. Dronskowski, D. Dzivenko, R. Riedel, U. Schwarz, *Chem. Mater.* **2009**, *21*, 392–398.
[19] R. Niewa, D. Rau, A. Wosylus, K. Meier, M. Wessel, R. Dronskowski, U. Schwarz, *J. Alloys Compd.*, in press.
[20] A. Leineweber, H. Jacobs, F. Hüning, H. Lueken, W. Kockelmann, *J. Alloys Compd.* **2001**, *316*, 21–38.
[21] K. H. Jack, *Acta Crystallogr.* **1952**, *5*, 404–411.
[22] T. Epicier, in: *The Physics and Chemistry of Carbides, Nitrides and Borides* (Ed.: R. Freer), **1990**, p. 215.
[23] R. Blachnik, in: *Taschenbuch für Chemiker und Physiker* (Eds.: D'Ans & Lax), part 3, Springer, Berlin, Heidelberg, New York, **1998**.
[24] The compressibility of media under extreme pressures: F. D. Murnaghan, *Prog. Natl. Acad. Sci. USA* **1944**, *30*, 244–247.
[25] D. Walker, M. A. Carpenter, C. Hitch, *Am. Mineral.* **1990**, *75*, 1020–1028.
[26] D. Walker, *Am. Mineral.* **1991**, *76*, 1092–1100.
[27] M. J. Walter, Y. Thibault, K. Wei, R. W. Luth, *Can. J. Phys.* **1995**, *73*, 273–286.
[28] D. C. Rubie, *Phase Transitions* **1999**, *68*, 431–451.
[29] D. A. Young, in: *Phase diagrams of the elements*, University of California Press, Berkeley, **1991**.
[30] L. Akselrud, *Image Integrator*, version 1.2, Max-Planck-Institut für Chemische Physik fester Stoffe, Dresden, **2005**.
[31] Use of the CSD program package for structure determination from powder data: L. G. Akselrud, P. Y. Zavalii, Yu. N. Grin, V. K. Pecharsky, B. Baumgartner, E. Woelfel, *Mater. Science Forum* **1993**, *133–136*, 335–340.
[32] a) G. Kresse, J. Hafner, *Phys. Rev. B* **1993**, *47*, 558–561; b) G. Kresse, J. Hafner, *Phys. Rev. B* **1994**, *49*, 14251–14269.
[33] a) G. Kresse, J. Furthmüller, *Comput. Mater. Sci.* **1996**, *6*, 15–50; b) G. Kresse, J. Furthmüller, *Phys. Rev. B* **1996**, *55*, 11169–11186.
[34] J. P. Perdew, K. Burke, M. Ernzerhof, *Phys. Rev. Lett.* **1996**, *77*, 3865–3868.
[35] P. E. Blöchl, *Phys. Rev. B* **1994**, *50*, 17953–17979.
[36] J. von Appen, R. Dronskowski, *Angew. Chem. Int. Ed.* **2005**, *44*, 1205–1210.
[37] A. Houben, P. Müller, J. von Appen, H. Lueken, R. Niewa, R. Dronskowski, *Angew. Chem. Int. Ed.* **2005**, *44*, 7212–7215.
[38] G. Sheldrick, C. Krüger, R. Goddard, *SHELXS-97*, University of Göttingen, Germany, **1985**.
[39] G. Sheldrick, **1997** *SHELXL97-2*, University of Göttingen, Germany, **1997**.

Received: December 18, 2008
Published Online: March 25, 2009

